INTER-AMERICAN TROPICAL TUNA COMMISSION

SCIENTIFIC ADVISORY COMMITTEE

13TH MEETING

(by videoconference)

16-20 May 2022

DOCUMENT SAC-13 INF-N

THE JAPANESE LOGBOOK ANALYSIS FOR THE SOUTH EASTERN PACIFIC OCEAN SWORDFISH ABUNDANCE INDICES USING R-INLA

Hirotaka Ijima[1], Carolina Minte-Vera and, Haikun Xu and Mark Maunder

ABSTRACT

We analyzed the logbooks recorded by the Japanese longline vessels to obtain the abundance index required for the south eastern Pacific Ocean (EPO) swordfish stock assessment. Considering the transition of Japanese longline fishing gear and the change of the logbook format, we separated the logbook into three time series (1975 to 1993, 1994-2009, 2010-2019). Using the R-INLA package, we constructed multiple GLMMs, including the spatiotemporal model, and selected the best model using the information criteria WAIC and LOO-CV. As a result of model selection, spatiotemporal models were selected for each time series. The standardized CPUE was estimated spatiotemporally, and the average value was calculated in a preset area. The standardization of CPUE also requires understanding the spatiotemporal distribution of the cohorts, and size and/or ages selected by the indices. GLMMs with the mean body weight of fish by set as the response variable were constructed to explore changes in sizes selected; a standardized spatiotemporal distribution of the mean body weight was obtained. Comparing the results of two GLMMs, we found that since 2001, a fishing ground has been formed offshore to the coastal area of Chile where Japanese longliners catch many small swordfish. These results will be helpful to understand the historical Japanese longline operation and the distribution pattern for the south Eastern Pacific swordfish stock.

INTRODUCTION

Standardized CPUE an essential information for stock assessment because it plays a role in tuning population dynamics trends in the stock assessment model. However, the swordfish CPUE obtained from the Japanese longline fishery in the eastern Pacific has shown a sharp increase in recent years, which may not be explained solely by the population dynamics (Hinton and Maunder 2011). The possibility that the CPUE increased sharply may be due to:

1. The catchability changed due to the change of fishing gear or target species.
2. The small fish catch increased due to a strong year class.
3. The size selectivity of the longline fishery changed due to changes in fishing gear.

To clarify these hypotheses, we first confirmed the historical transition of the Japanese longline fishery and the operation style depending on the fishing ground. Next, we illustrated the spatiotemporal variation in nominal CPUE and in the average weight of the swordfish and investigated the spatial distribution of small fish. Based on these background analyses, we constructed a GLMM that considers spatiotemporal effect using the R-INLA package. The output of latent spatial fields can help understand potential spatiotemporal effects such as environmental factors. The resulting standardized CPUE for the EPO is shown as aggregated in for four areas roughly corresponding to regions with different size composition (Figure. 1).

MATERIAL AND METHODS

Japanese longline logbook data

Changes in logbook data

The Japanese longline fishery has a very long history, and the oldest catch statistics by this fishery are from the 1920s (Okamoto 2004). After World War II, with the abolition of the MacArthur line in 1952, a modern longline fishing logbook based on Japanese law was implemented (Okamoto 2004). The logbook reported the fishing location, catch numbers by species, and effort in numbers of hooks, making it possible to calculate the number of fish caught per unit effort (CPUE). Since 1952, the longline logbook data has gradually changed in format. The most significant changes in the logbooks were in 1975 and 1994. In 1975, information on hooks between floats (HPB) was added. Since 1994, fields regarding details on the gear configuration and catch in weight have been added, and it has become possible to understand the fishing operation patterns more fully. In this paper, we used the catch reports from 1976 on, because since then the logbook database contains the name of the fishing vessel.

The spatiotemporal transition of fishing gear in the longline fishery

Between 1976 and 2019, the Japanese longline fishery has been changing its style of operation. For example, HBF increased in stages (Figure 2). It is generally believed that high HBF causes the deep sinking of bait and changes in catchability between species distributed at different depths (Ward and Hindmarsh 2007), thus the HBF information could be used as a proxy for the fishing depth. However, comparing HBFs trends over a long period has to be done with caution, due to other changes in the gear that may influence the fishing depths. In the mid-1990s, the mainline and branch line material changed from natural fibers such as hemp to nylon, and the total gear weight became significantly lighter (Figures 3 and 4). Due to the different weights between the same HBF in the 1970s and in the 2000s, the gear does not always sink to the same depth. The number of branch lines has increased since 1994, which is thought to have the purpose to sink the lighter line deeper.

Japanese longliners have also changed their fishing gear settings depending on the fishing ground. In the coastal area of the eastern Pacific Ocean (EPO) south of 10°S, the HBF is low, and the length between branch lines and the length of the buoy lines tend to be shorter (Figure 5-7, see also SAC-04-04b). In other words, it is considered that fishing gear is set to keep the fishing depth shallow in these areas.

Light sticks may have been introduced around 2010. At present, there are not enough data regarding the use of light sticks by the Japanese fleet, but it is thought that this will have a significant impact on the catchability of swordfish. Furthermore, due to the recent decrease in the bigeye catch, it seems that some vessels have shifted their targeting to swordfish. However, there is no data on targeting practices of the Japanese fleet.

In this way, the catchability based on fishing gear is expected to have spatiotemporal changes. Thus, statistical analysis for the Japanese longline logbook data is problematic. Specifically, when we treat the gear effect as categorical data in the GLMM, sets with old and new gear are needed at the same time to be able to estimate the effect of that gear change. However, no such data is available. Considering this issue, we decided to divide the Japanese logbook data into three time series, 1976-1993, 1994-2009, and 2010-2019, and carry out standardization separately for these three periods.

Nominal CPUE and mean body weight by sets

Before the analysis by statistical models, we confirmed spatiotemporal variation in nominal CPUE of fish per 1,000 hooks (Figure 7). Since the 2000s, fishing grounds have shrunk significantly, and overall CPUE has risen (Figure 7). Specifically, the fishing ground where CPUE> 2 is different around the 2000s, and since the 2000s it is consistent with where fish weighing less than 30 kg on average are caught (Figures 7 and 8). Looking at the number of fish caught by three time series, the zero-catch rate has decreased significantly since 2010 (Figure. 9). The smallest in average weight tended to be in area “3. Coastal” in the fourth quarter, while the largest to be in area “1.EquatorialN” in the second and third quarters (Figure 10). There was no apparent difference in other cases.

Spatiotemporal GLMM

We used the R software package, R-INLA (Lindgren and Rue 2015), for the CPUE standardization and constructed a generalized linear mixed model (GLMM) considering the spatiotemporal effect and examined the combination of multiple fixed effects. The catch in numbers by set was assumed to have a zero-inflated Poisson distribution, and the effort was added as an offset. The spatiotemporal GLMM is

$C_i \sim ZIP(\mu_i, \pi)$,

$E(C_i) = \mu_i(1-\pi)$,

$Var(C_i) = \mu_i(\mu_i + \pi\mu_i^2)$ and,

$\log(\mu_i) = \mathbf{X}_i\boldsymbol{\beta} + \mathbf{Z}_i\boldsymbol{\delta}_i + \mathbf{A}_i\mathbf{u} + \log(1{,}000 hooks_i)$.

Where C_i is number of swordfish catch by set *i*, μ_i is the mean value of swordfish catch by set *i*, π is the probability of zero catch, $\mathbf{X}_i$ is the covariate matrix row in the set *i*, $\boldsymbol{\beta}$ are fixed effect coefficients vector for each covariates. $\mathbf{Z}_i$ is the model matrix row for the random effects in set *i* and $\boldsymbol{\delta_i}$ is the random effect coefficients vector that is $\boldsymbol{\delta}_i \sim \mathbf{N}(\mathbf{0}, \boldsymbol{\Psi})$, where $\boldsymbol{\Psi}$ is the covariance matrix that depends on number of random effects variables. $\mathbf{A}_i$ is a projector matrix row in the set *i*, and $\mathbf{u}$ is a spatial effect.

The elements of spatial effect in location *s* on year *t* ($u_{s,t}$) follows AR1 process as

$u_{s,t} = \rho u_{s,t-1} + v_{s,t}$, where ρ is an auto-correlation parameter $v_{s,t}$ is a spatial Gaussian random field $v_{s,t} \sim GMRF(0, \Sigma)$. The elements of covariance is $\Sigma_{j,k} = \sigma_v^2 Cor_M\left(v(s_j), v(s_k)\right)$ and correlation function is the Matérn correlation function

$$Cor_M\left(v(s_j), v(s_k)\right) = \frac{2^{1-\nu}}{\Gamma(\nu)}\left(\kappa\|s_j - s_k\|\right)^{\nu} \mathrm{K}_\nu\left(\kappa\|s_j - s_k\|\right).$$

We examined simple spatial GLMMs and more complicated models such as a spatiotemporal (AR4) GLMM that considered seasonality.

Similar to the approach for CPUE, we constructed a spatiotemporal GLMM for the average weight and estimate the spatiotemporal variation in individual weight of swordfish caught.

The average weight model is

$$\log(W_i) = N(\mu_i, \sigma^2)$$

$$\log(\mu_i) = \mathbf{X}_i\boldsymbol{\beta} + \delta_i + \mathbf{A}_i\mathbf{u}.$$

Where W_i is mean body weight of swordfish by set *i*, $\mathbf{X}_i$ is the covariate matrix row in the set *i*, $\boldsymbol{\beta}$ are coefficients vector for each covariates, δ_i is the random effect given by vessel name, $\mathbf{A}_i$ is a projector matrix row in the set *i*, and $\mathbf{u}$ is a spatial effect considering AR1 process and that is same as the CPUE model. The mean body weight model did not use zero-catch data because we never know the fish size of zero catch situation.

R-INLA estimates the posterior of parameters using Bayesian inference. The prior coefficient vector for each covariate (***β***) was set as a default value of the INLA package's Gaussian prior. We used the half-Cauchy distribution truncated at zero to serve as a prior for the standard deviation sigma. Penalized Complexity (PC) priors were used for the spatial effects parameters, auto-correlation parameter and probability of zero catch. The practical range and marginal deviation were used for spatial effects parameters (Krainski et al 2018, Fuglstad et al 2019).

The list of models examined is shown in Table.1.

Model selection

It is known that AIC cannot be used to select among complex models, such as random effect models and hierarchical models (Watanabe 2010). Since R-INLA used Bayesian inference, both Widely Applicable and Bayesian Information Criterion (WAIC) and Leave One Out Cross Validation (LOOCV) can be calculated (Watanabe 2010, Vehtari et al., 2017). In this study, model selection was performed using WAIC and LOOCV, and the value of over dispersion was also confirmed. WAIC and LOOCV can also evaluate which prior is the better prediction performance, but this study did not check the prior effect.

Standardized CPUE

Standardized CPUE was calculated using the estimated fixed effect parameters and the potential spatial field. The indices for each area and period were area-weighted; they were computed using the sum of the estimated CPUE for each 1° of latitude by 1° of longitude cell for which there was one or more observation. These calculations avoid giving the cell with more sets a disproportionate weight in the indices.

RESULTS AND DISCUSSION

As a result of model selection using WAIC and LOOCV, spatiotemporal models were selected for the three time series (Table. 2). The effect of the spatial field might be accompanied by seasonality. However, we left this work for the future because often this complicated model crashed R and did not converge even after two or more weeks. The estimated latent spatial field showed temporal change, and since 2001 a significant positive spatial field has appeared in the coastal area (Figure. 11-13). When looking at the spatially standardized CPUE and latent spatial field, there is a high-density area in 1978 off the coast of Panama (Figure 14 and 17). This estimate may be lower because no high CPUE has been observed in this area. Furthermore, R often crashed for the early time series, and the estimation quality may be low because the older logbook data might be inaccurate. Thus, we need to address data screening again in the future. The spatial distribution of CPUE during the mid and late time series was higher in the coastal area after 2001, similar to the latent spatial field (Figures 15 and 16). This high-density area significantly affected the current CPUE trend. When the CPUEs estimated in these spatiotemporal areas were averaged for each area, they showed temporal changes that were generally similar to the nominal CPUEs except for the coastal area (Figure. 17-19).

Near the equator from 10°N to 10°S, the spatial field fluctuated wildly by year. For example, in 1994, 1995, 1998, and 1999, negative areas spread widely, but positive effects were estimated in other years (Figures 20 and 21). Due to such changes in the spatial field, the standardized mean body weight also fluctuated spatiotemporally. Especially near the equator, the difference is more extensive than in other areas (Figure. 22-23). On the other hand, Japanese longlines have caught small swordfish throughout the coastal waters (Figures 22-23). These results are generally consistent with high CPUE waters, suggesting that high CPUE in these areas are due to large quantities of small swordfish.

REFERENCES

Fuglstad, G.A., Simpson, D., Lindgren, F. and Rue, H., 2019. Constructing priors that penalize the complexity of Gaussian random fields. Journal of the American Statistical Association, 114(525), pp.445-452.

Krainski, E., Gómez-Rubio, V., Bakka, H., Lenzi, A., Castro-Camilo, D., Simpson, D., Lindgren, F. and Rue, H., 2018. Advanced spatial modeling with stochastic partial differential equations using R and INLA. Chapman and Hall/CRC.

Okamoto, H., 2004 Search for the Japanese tuna fishing data before and just after World War II (in Japanese). Bulletin of Fisheries Research Agency, 13, pp.15-34.

Lindgren, F. and Rue, H., 2015. Bayesian spatial modelling with R-INLA. Journal of Statistical Software, 63(19), pp.1-25.

Vehtari, A., Gelman, A. and Gabry, J., 2017. Practical Bayesian model evaluation using leave-one-out cross-validation and WAIC. Statistics and computing, 27(5), pp.1413-1432.

Ward, P. and Hindmarsh, S., 2007. An overview of historical changes in the fishing gear and practices of pelagic longliners, with particular reference to Japan's Pacific fleet. Reviews in Fish Biology and Fisheries, 17(4), pp.501-516.

Watanabe, S., 2010. Asymptotic equivalence of Bayes cross validation and widely applicable information criterion in singular learning theory. Journal of machine learning research, 11(12).

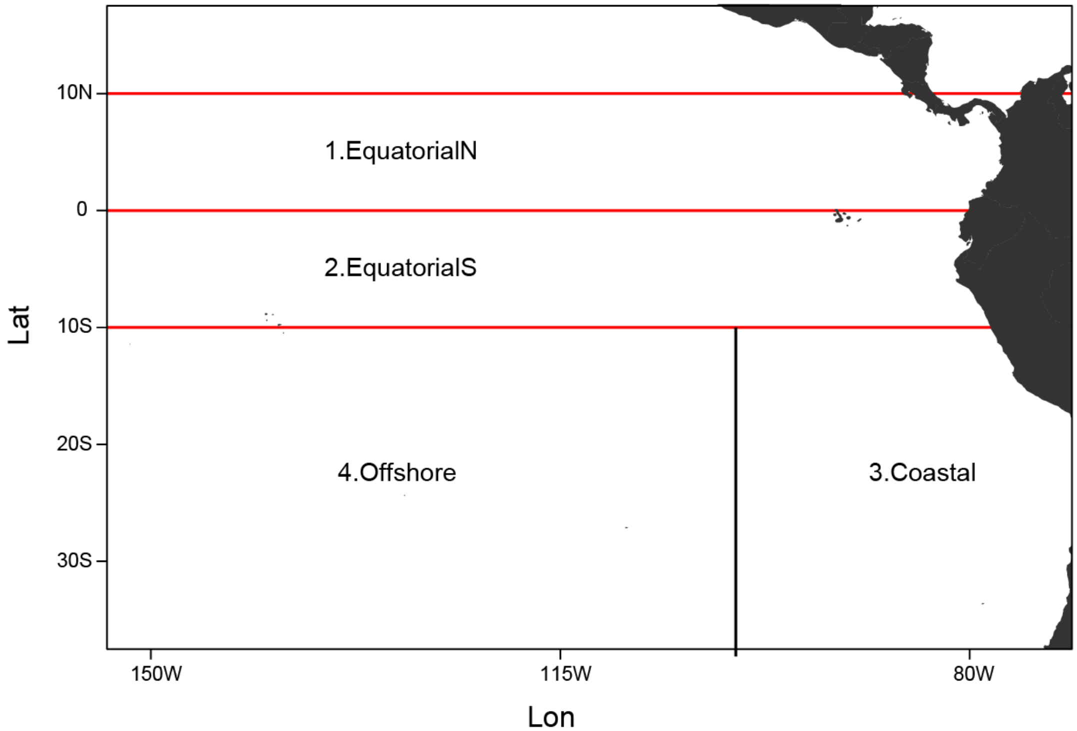

FIGURE 1. Area definitions for this study.

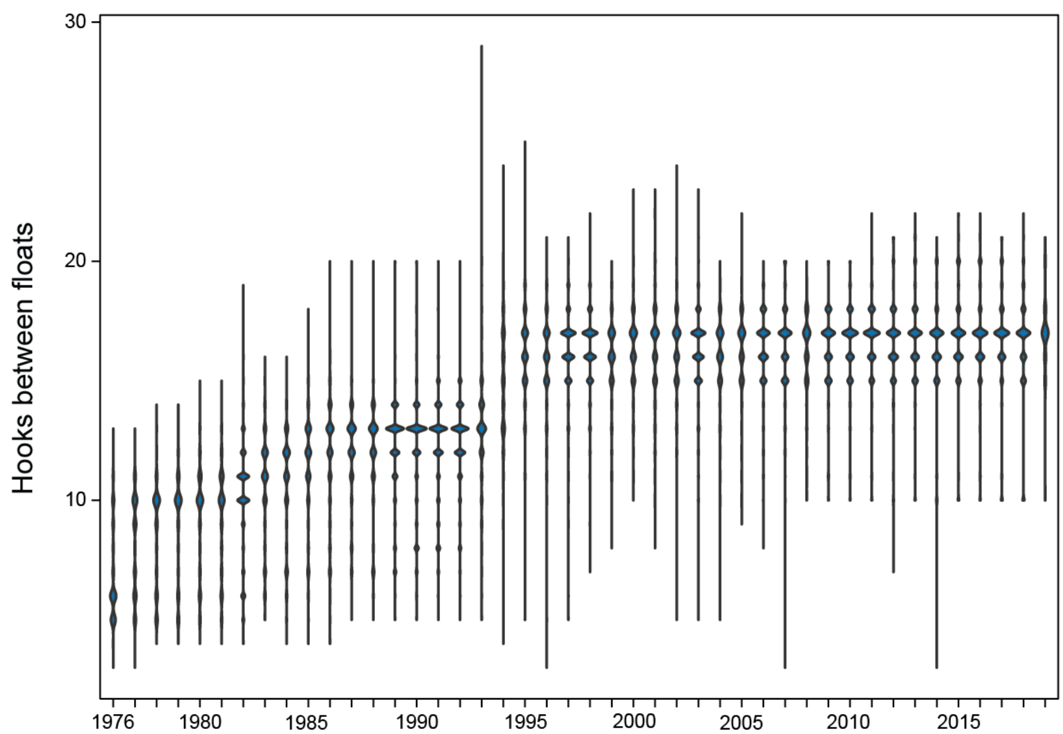

FIGURE 2. Historical changes in gear configuration (hooks between floats) of Japanese longline fishery in the Eastern Pacific Ocean.

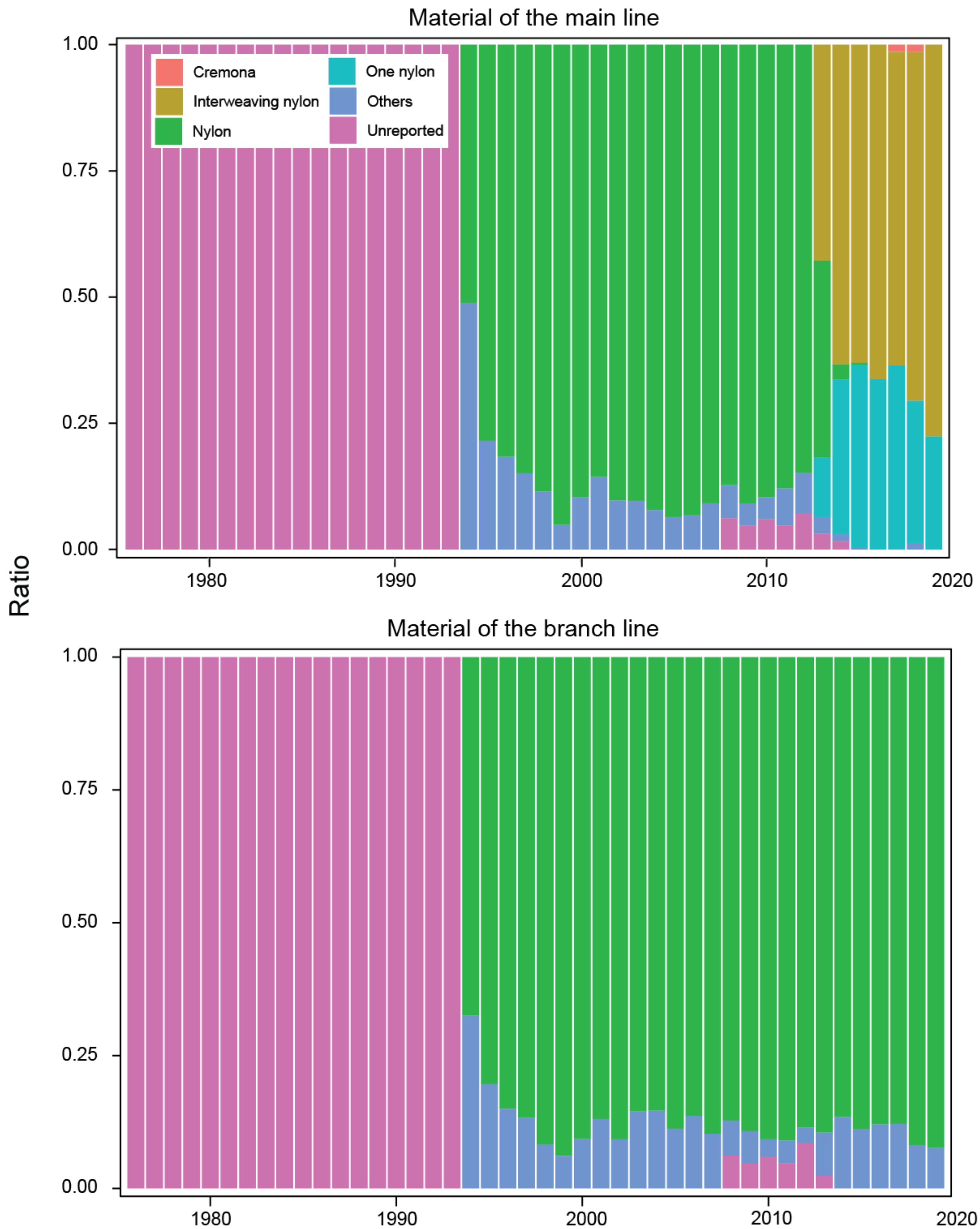

FIGURE 3. Historical changes in gear configuration of Japanese longline fishery (material of the main line and materials of the branch line). It is considered that others are natural materials such as hemp line.

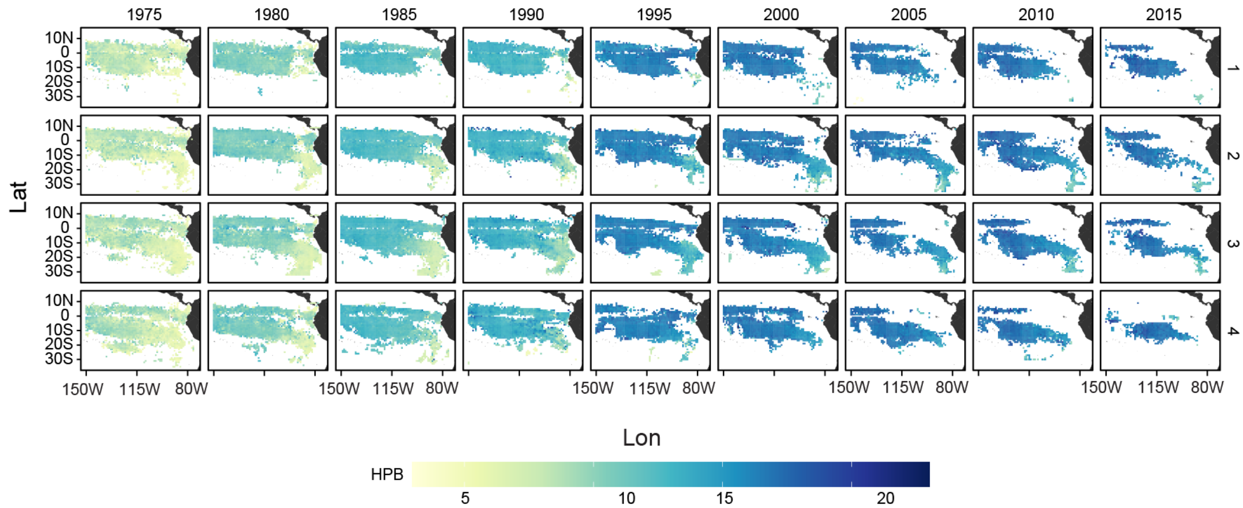

FIGURE 4. The spatiotemporal trend of the hooks between floats by groups of 5 years and by quarter.

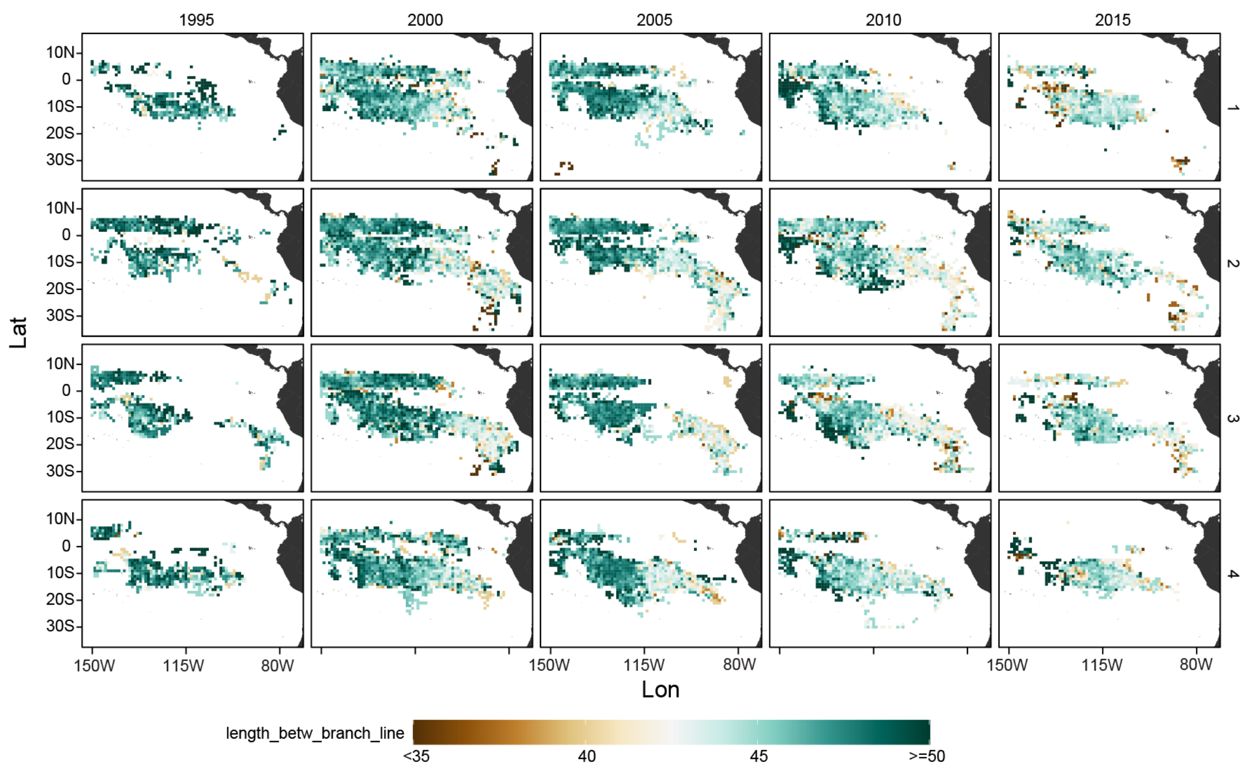

FIGURE 5. The spatiotemporal pattern of the branch line length for Japanese longline fishery by groups of 5 years and by quarter.

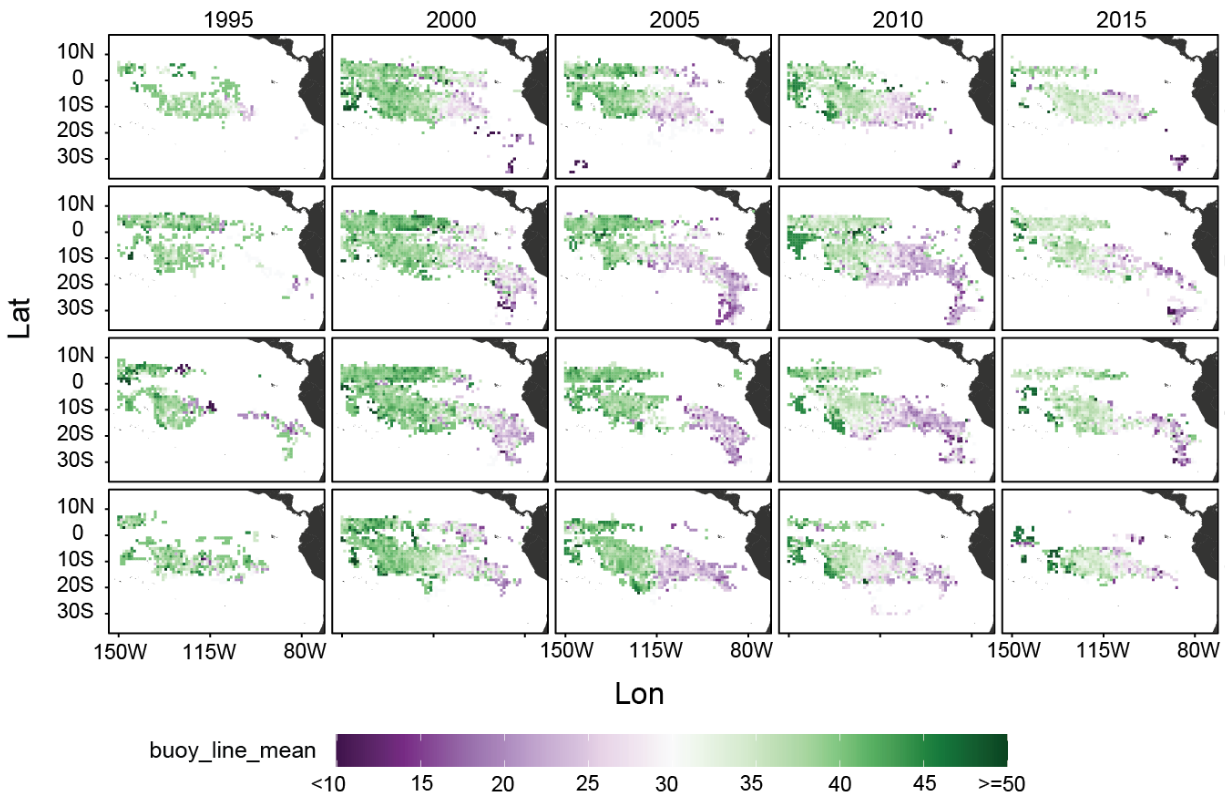

FIGURE 6. The spatiotemporal pattern of the buoy line length for Japanese longline fishery by groups of 5 years and by quarter.

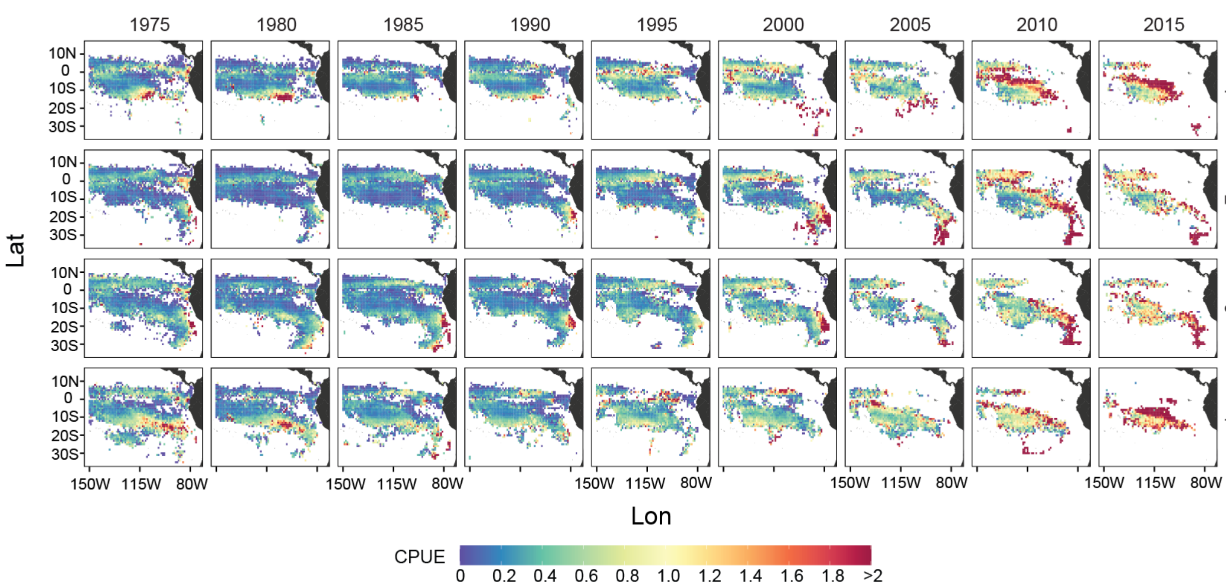

FIGURE 7. The spatiotemporal changes in swordfish nominal CPUE (number of fish / 1000 hooks) by groups of 5 years and by quarter.

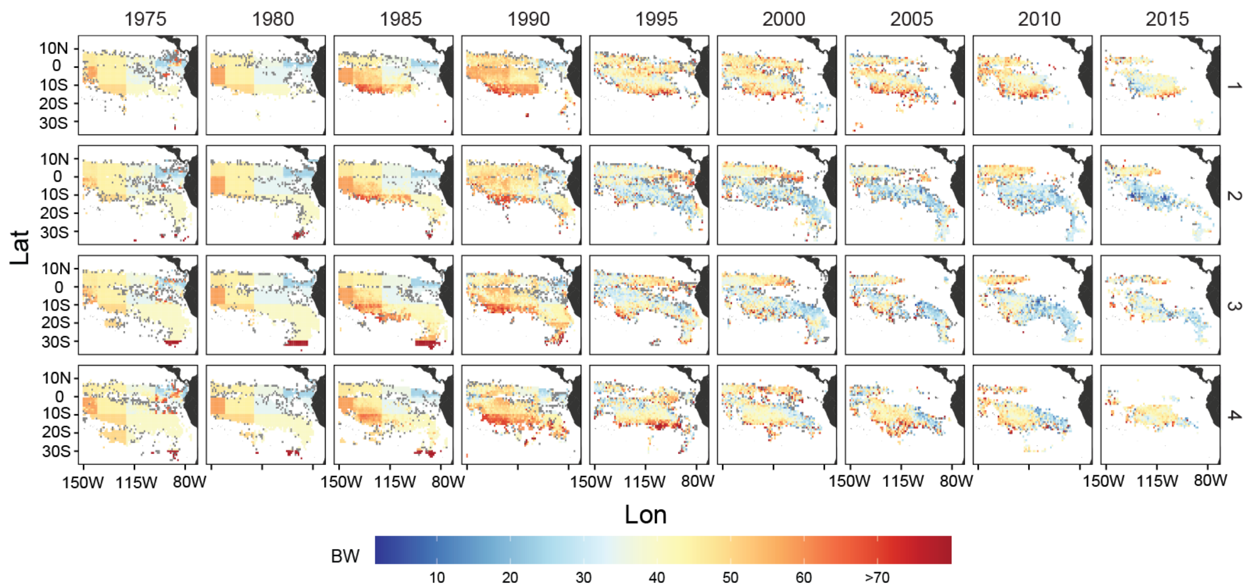

FIGURE 8. The spatiotemporal changes in the mean body weight (semi-dress weight) of swordfish caught by Japanese longline fishery by groups of 5 years and by quarter. Before 1994, There are no logbook data for the catch in weight by sets.

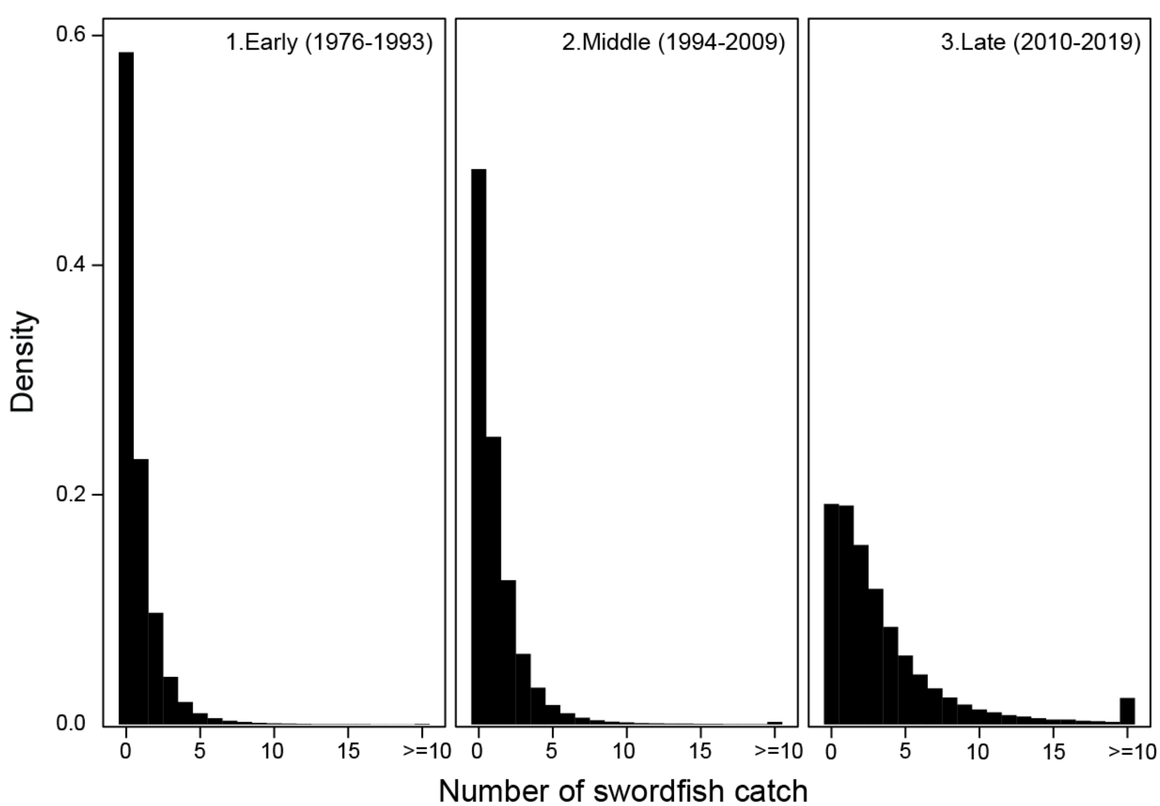

FIGURE 9. Number of swordfish caught by Japanese longline fishery summarized by set.

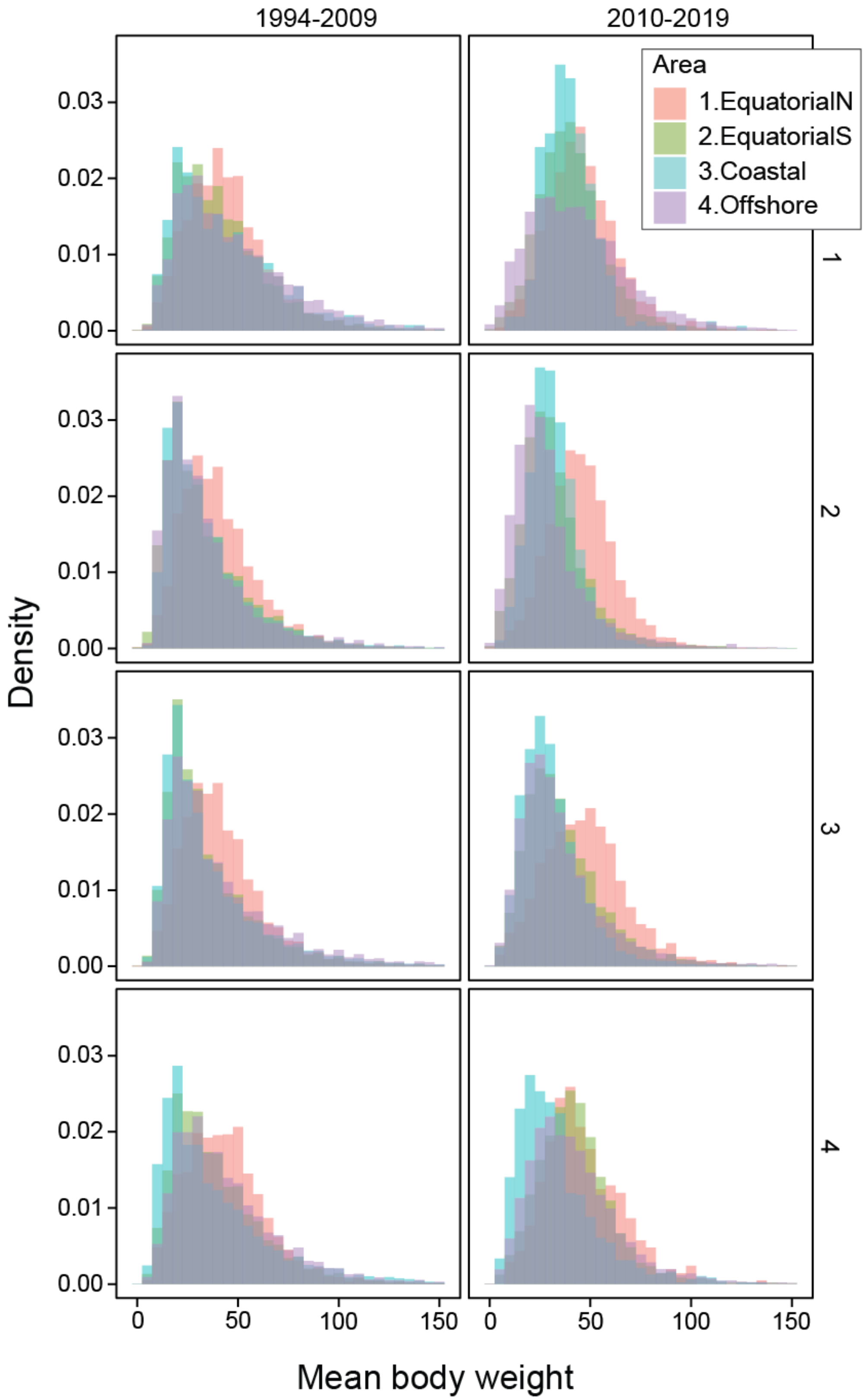

FIGURE 10. Distribution of mean body weight by set of swordfish by area.

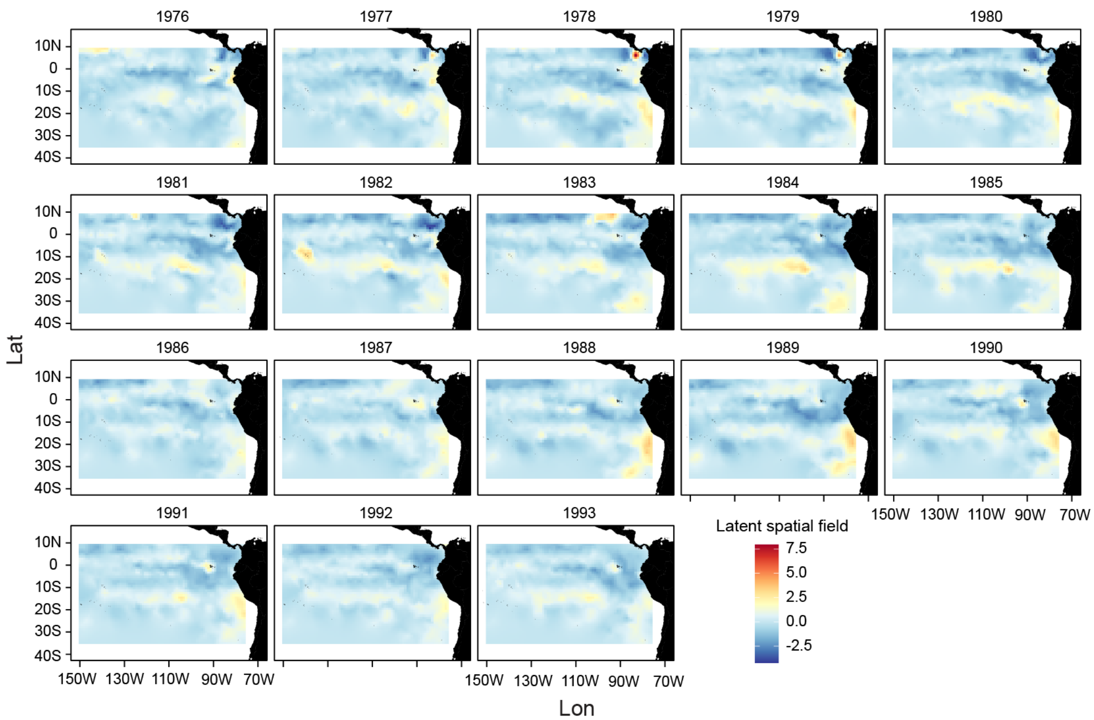

FIGURE 11. The latent spatial field estimated by catch number model (1976-1993).

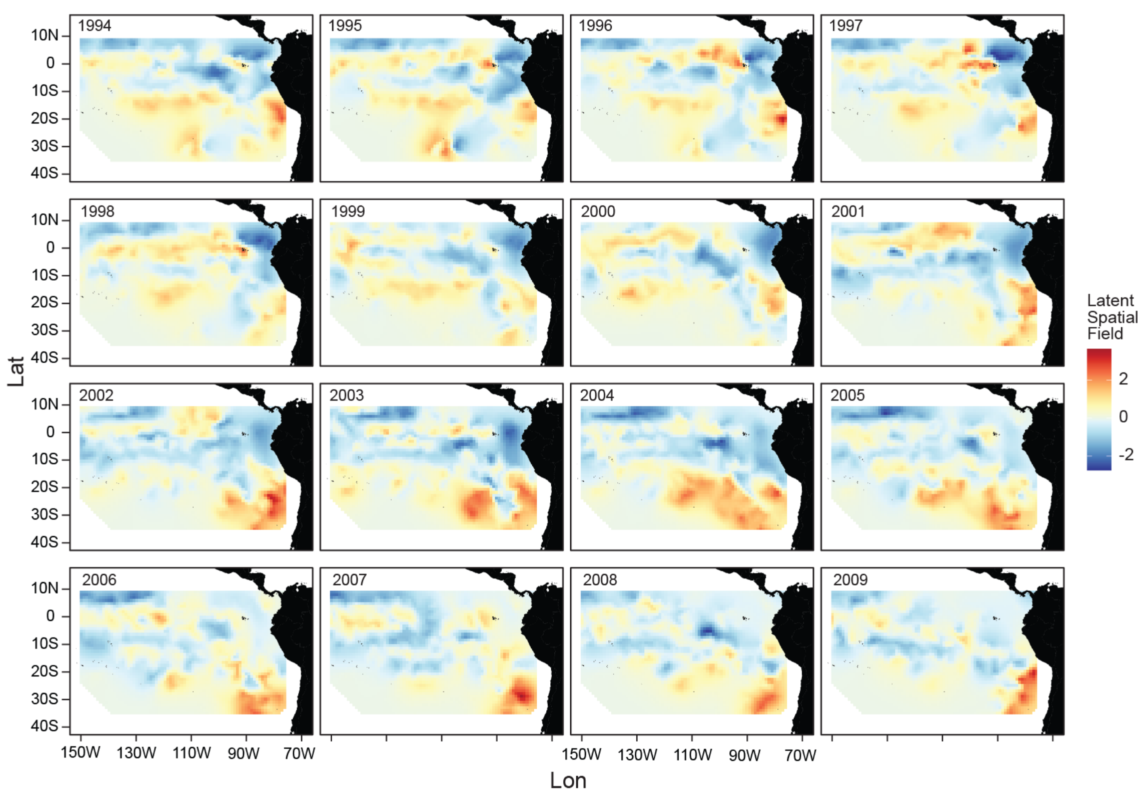

FIGURE 12. The latent spatial field estimated by catch number model (1994-2009).

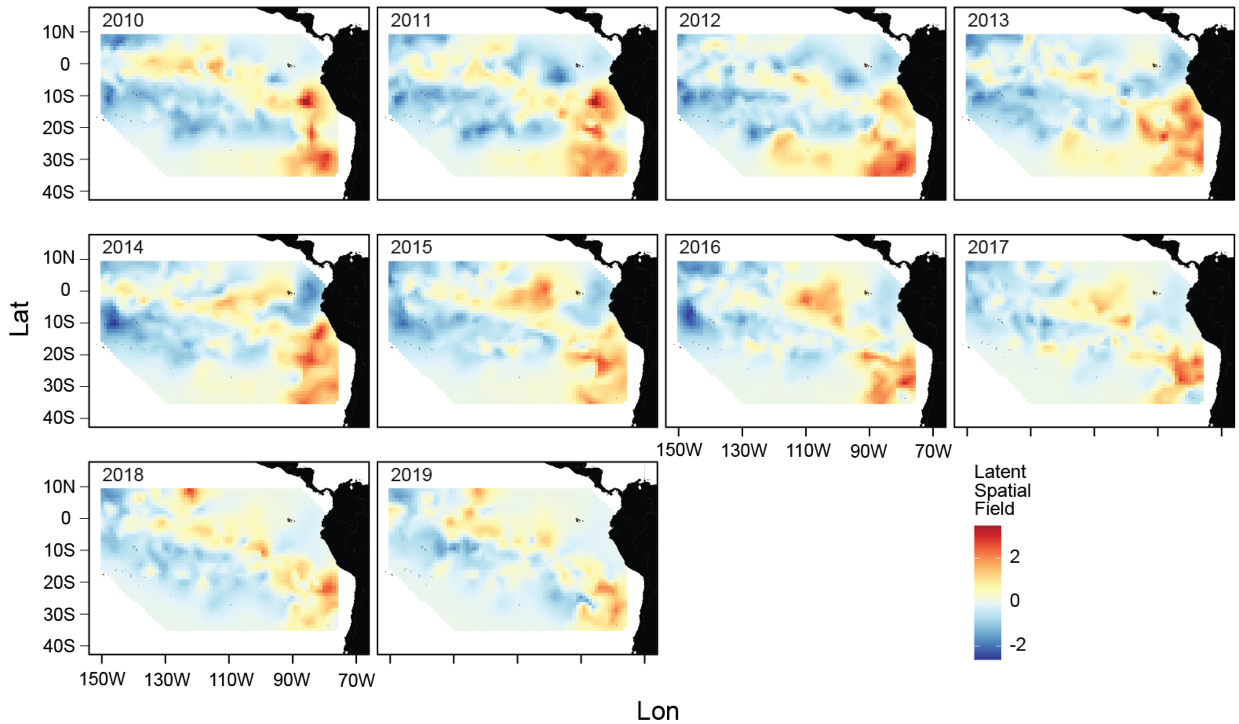

FIGURE 13. The latent spatial field estimated by catch number model (2010-2019).

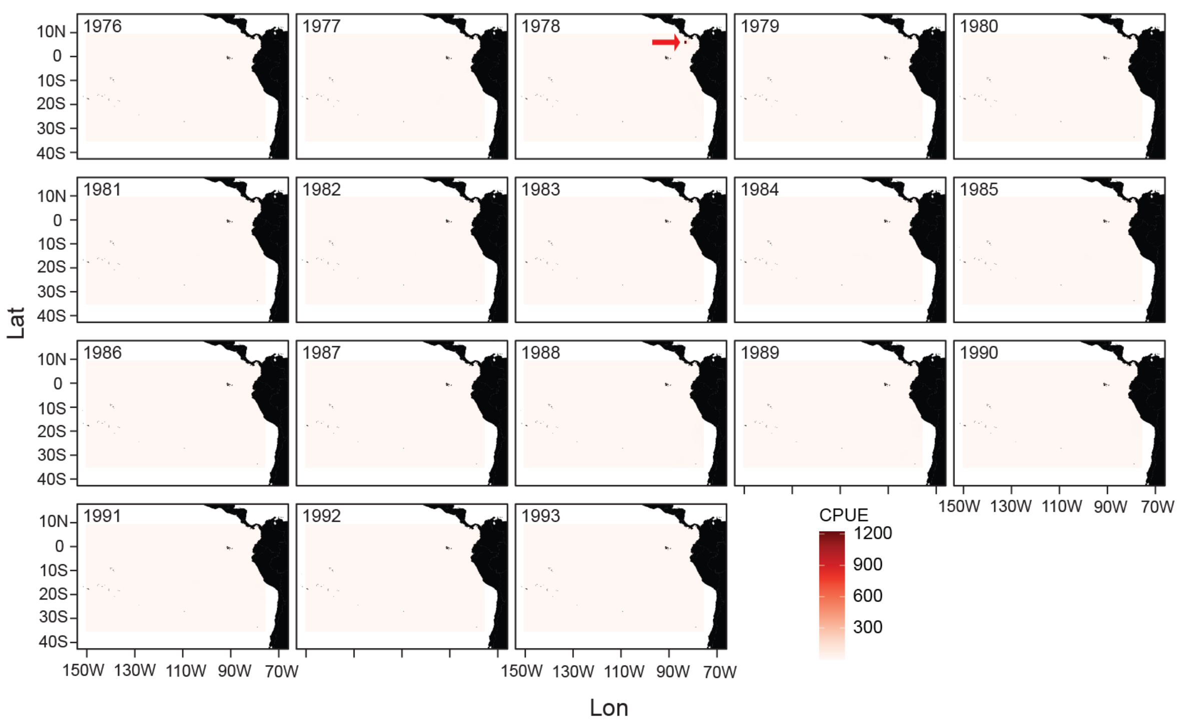

FIGURE 14. The standardized swordfish CPUE caught by the Japanese longline fishery (1976-1993). There is a small area (red arrow) where has a significantly large CPUE in 1978.

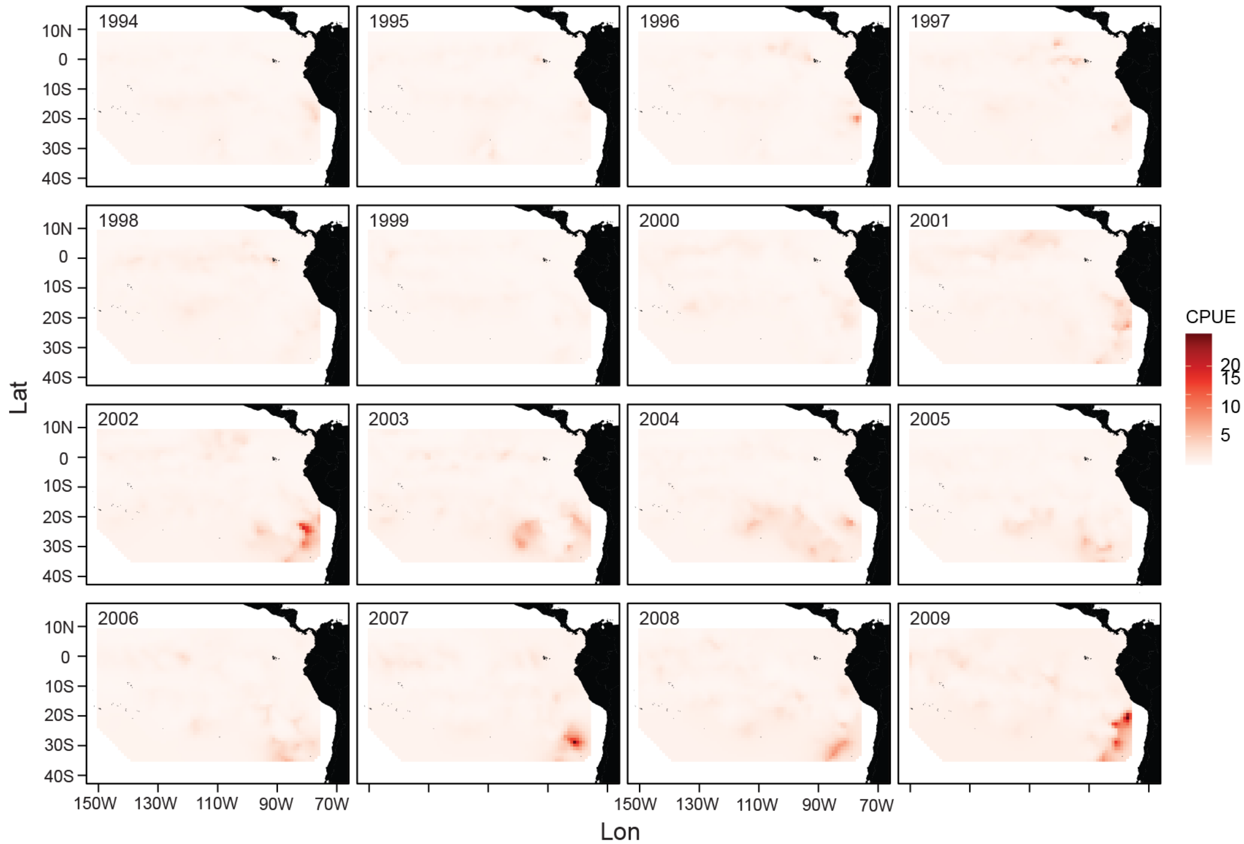

FIGURE 15. The standardized swordfish CPUE caught by the Japanese longline fishery (1994-2009).

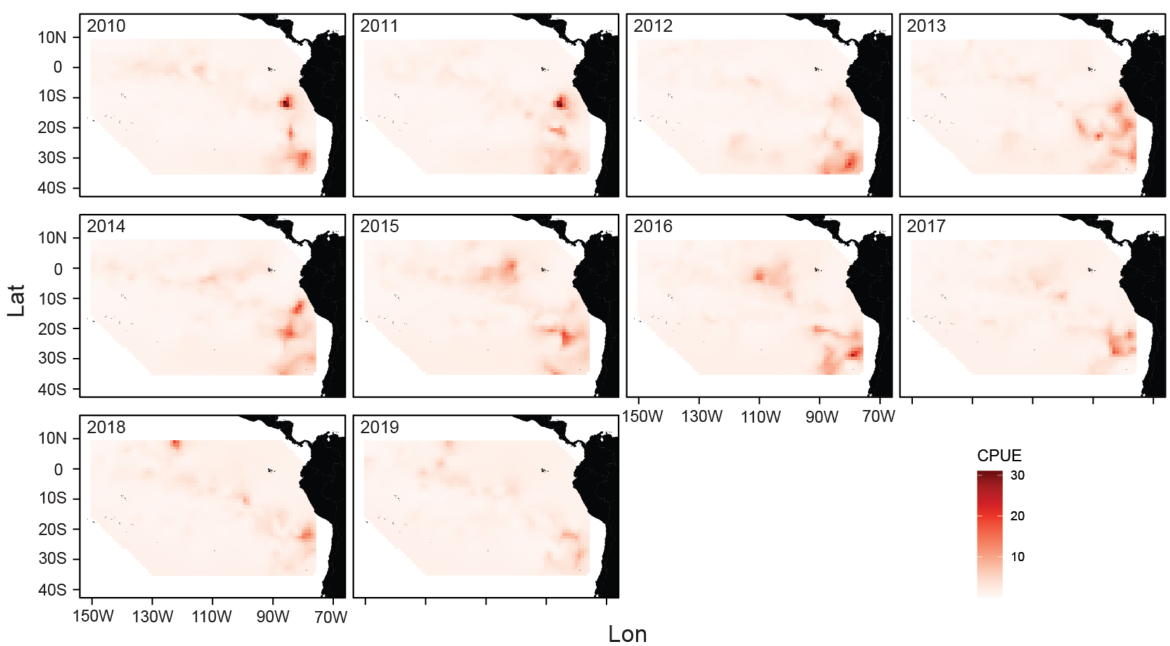

FIGURE 16. The standardized swordfish CPUE caught by the Japanese longline fishery (2010-2019).

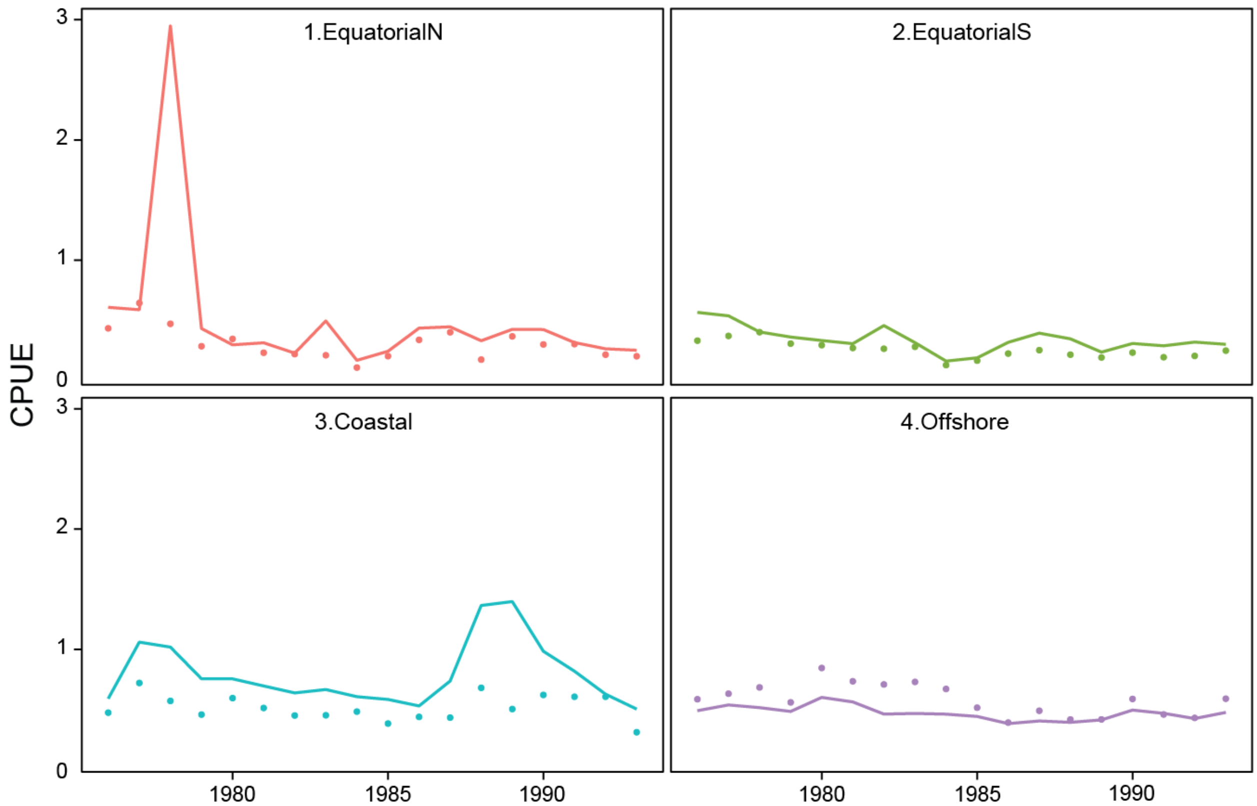

FIGURE 17. The standardized swordfish CPUE summarized by area (1976-1993). The solid line denotes standardized CPUE and points are nominal CPUE respectively.

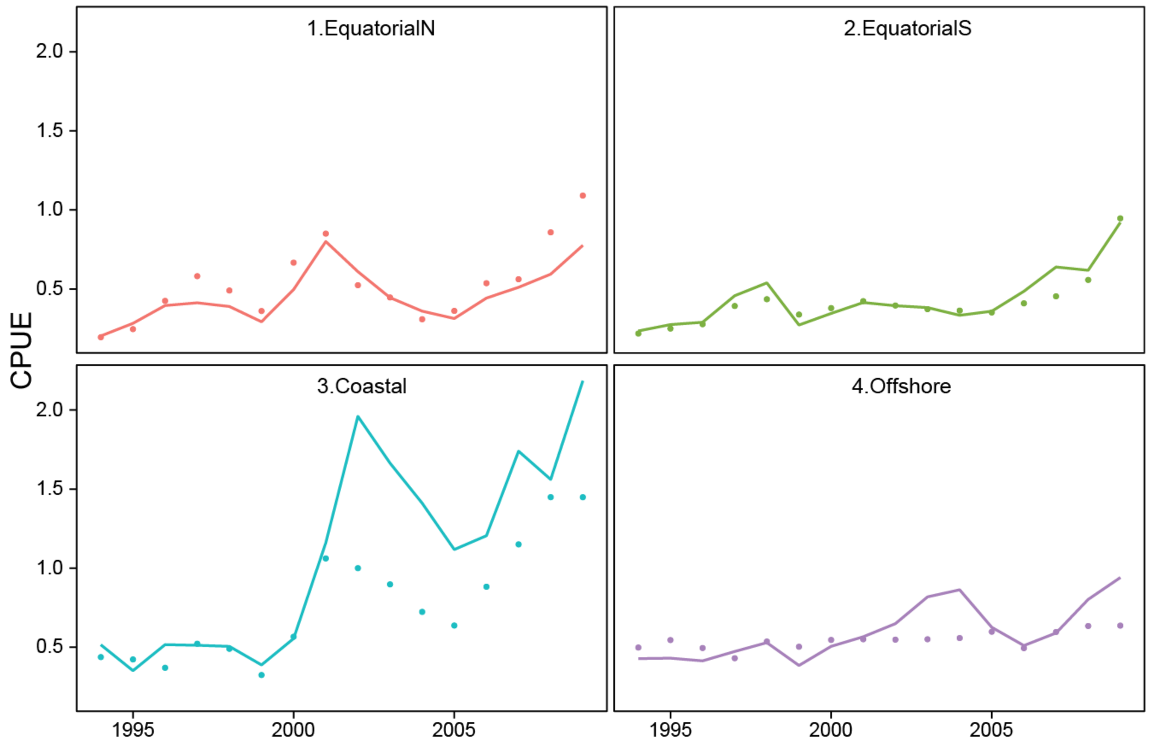

FIGURE 18. The standardized swordfish CPUE summarized by area (1994-2009). The solid line denotes standardized CPUE and points are nominal CPUE respectively.

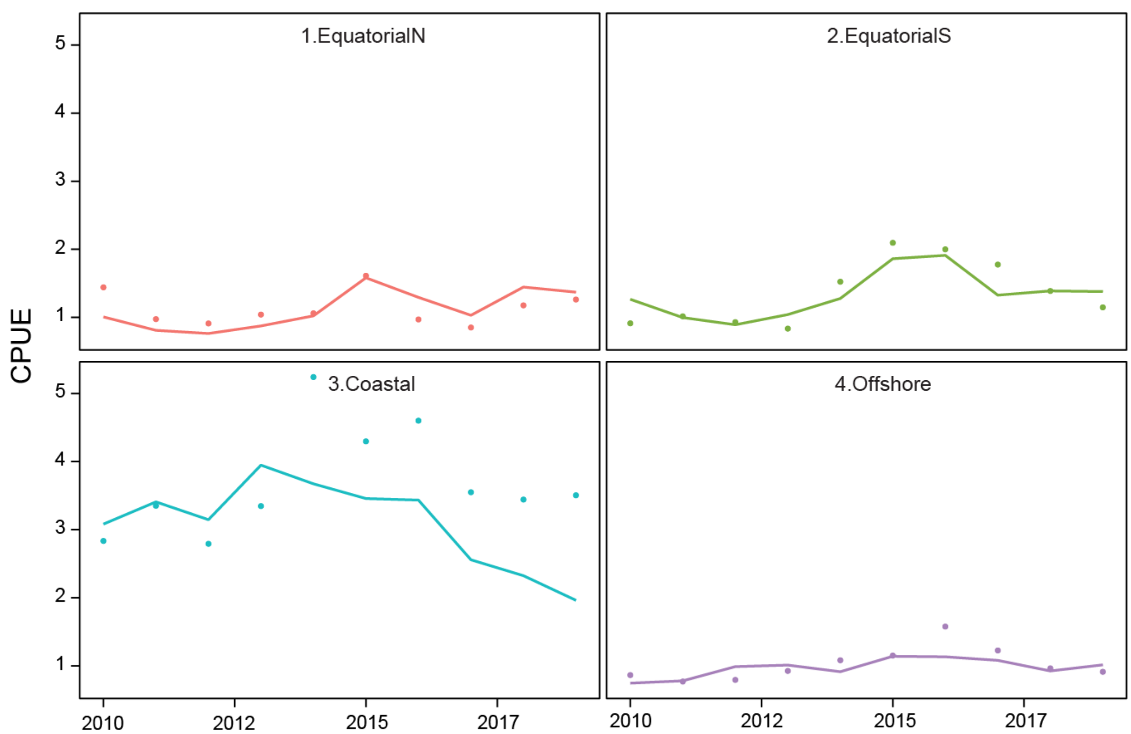

FIGURE 19. The standardized swordfish CPUE summarized by area (2010-2019). The solid line denotes standardized CPUE and points are nominal CPUE respectively.

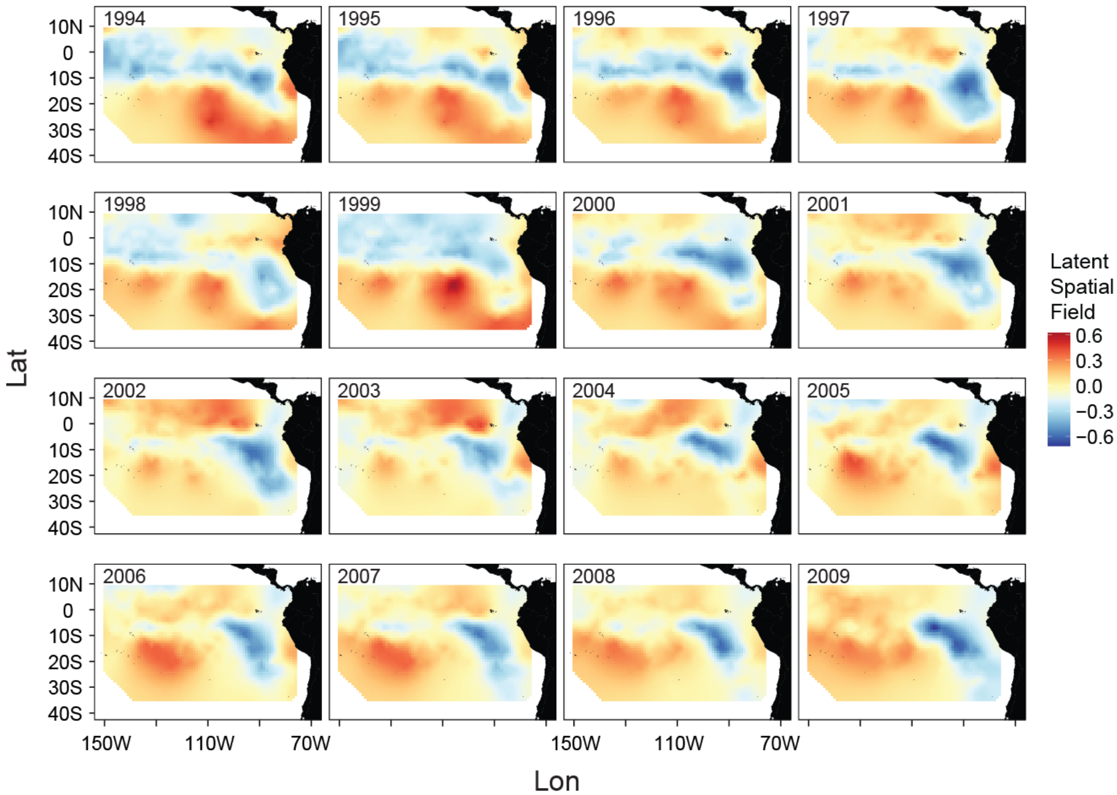

FIGURE 20. The latent spatial field estimated by mean body weight model (1994-2009).

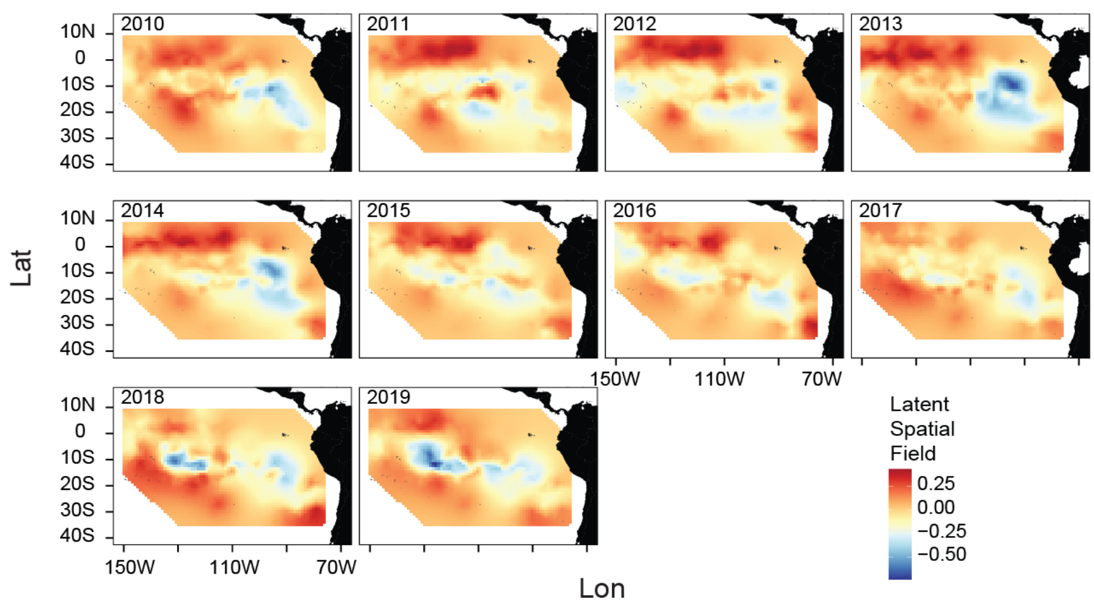

FIGURE 21. The latent spatial field estimated by mean body weight model (2010-2019).

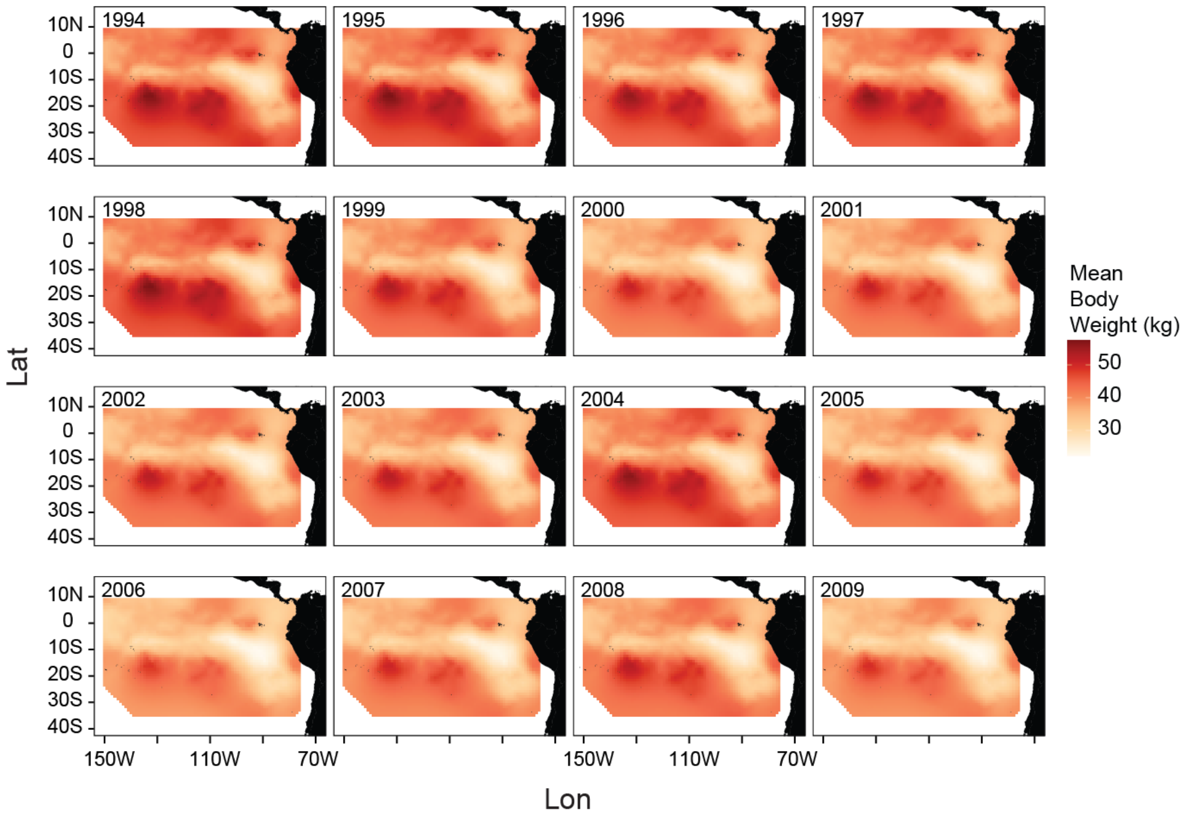

FIGURE 22. The standardized mean body weight of swordfish by set by set (1994-2009).

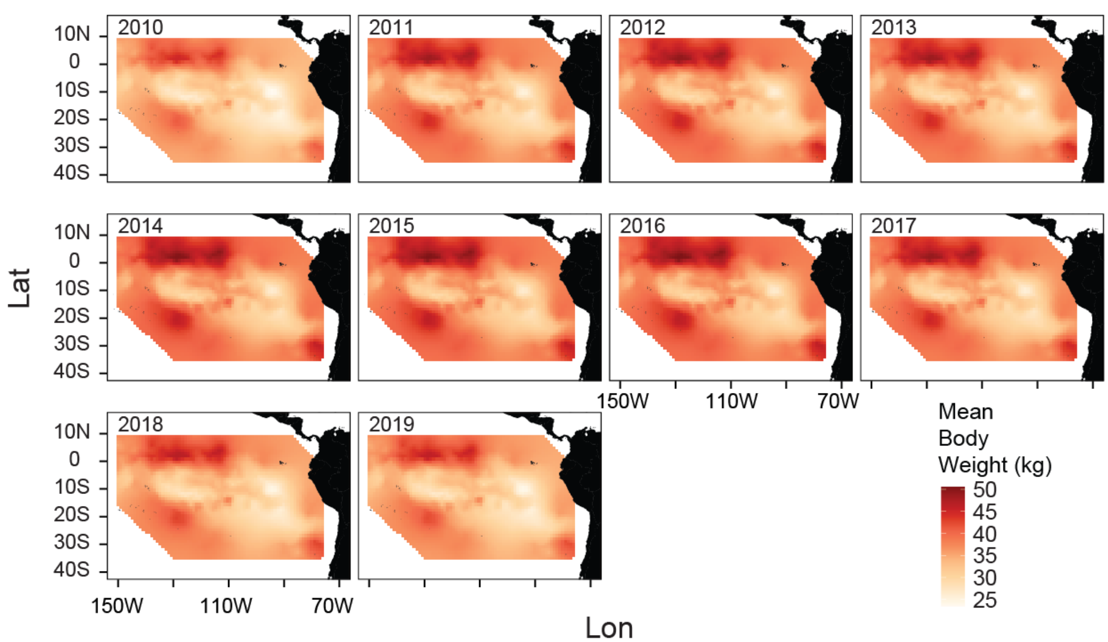

FIGURE 23. The standardized mean body weight of swordfish by set by set (2010-2019).

TABLE 1. Candidate GLMMs for the stock abundance indices of swordfish in the eastern Pacific Ocean

No	Time period	Model name	Model description in R-INLA	Distribution	Link	Remarks
1	2010-2019	po_sptime_yrqtr	swo~-1+yr+qtr+f(ves_eff, model='iid', hyper=hcprior)+f(w, model=spde, group=w.group, control.group=list(model='ar1', hyper=h.spec))+log(hooks/1000)	Po	Log	Data was "not" aggregated
2	2010-2019	po_sptime_allcov	swo~-1+yr+qtr+f(hpb, model='iid', hyper=hcprior)+f(ves_eff, model='iid', hyper=hcprior)+f(w, model=spde, group=w.group, control.group=list(model='ar1', hyper=h.spec))+log(hooks/1000)	Po	Log	Data was "not" aggregated
3	2010-2019	zip_sptime_yr	swo~-1+yr+f(w, model=spde, group=w.group, control.group=list(model='ar1', hyper=h.spec))+log(hooks/1000)	ZIP	Log	Data was "not" aggregated
4	2010-2019	zip_sptime_allcov1	swo~-1 + yr+qtr+hpb+f(ves_eff, model='iid', hyper=hcprior)+f(w, model=spde, group=w.group, control.group=list(model='ar1', hyper=h.spec))+log(hooks/1000)	ZIP	Log	Data was "not" aggregated
5	2010-2019	zip_sptime_allcov1_rev1	swo~-1+yr+qtr+hpb+f(ves_eff, model='iid', hyper=hcprior)+f(w, model=spde, group=w.group, control.group=list(model='ar1', hyper=h.spec))+log(hooks/1000)+log(hooks/1000)	ZIP	Log	Data was "not" aggregated Doropped HPB=3 and 7 (n=2 sets), Selected model
6	2010-2019	zip_sptime_allcov2	swo~-1+yr+qtr+f(hpb, model='iid', hyper=hcprior)+f(ves_eff, model='iid', hyper=hcprior)+f(w, model=spde, group=w.group, control.group=list(model='ar1', hyper=h.spec))+log(hooks/1000)	ZIP	Log	Data was "not" aggregated
7	2010-2019	zip_sptime(ar4)_allcov	swo ~-1+yr+f(hpb, model="iid", hyper=hcprior)+f(ves_eff, model="iid", hyper=hcprior)+f(w, model=spde, group=w.group, control.group=list(model="ar", order=4, hyper=h.spec))+log(hooks/1000)	ZIP	Log	Calculation did not finish even after 10 days work.
8	2010-2019	zip_sptime_allcov3	swo~-1+yr+qtr+hpb+f(ves_eff, model='iid', hyper=hcprior)+f(w, model=spde, group=w.group, control.group=list(model='ar1', hyper=h.spec))+f(w2, model=spde, group=w2.group, control.group=list(model="iid"))+log(hooks/1000), w=year, w2=season	ZIP	Log	Doropped HPB=3 and 7 (n=2 sets), Selected model, Data was aggregated by yr, qtr, lat, lon, hpb, and vessel name.
9	2010-2019	zip_sptime_allcov1_rev2	swo~-1+yr+qtr+hpb+f(ves_eff, model='iid', hyper=hcprior)+f(w, model=spde, group=w.group, control.group=list(model='ar1', hyper=h.spec))+log(hooks/1000)	ZIP	Log	Doropped HPB=3 and 7 (n=2 sets), Selected model, Data was aggregated by yr, qtr, lat, lon, hpb, and vessel name.
10	2010-2019	zip_sptime(ar4)_allcov_rev1	swo ~-1+yr+f(hpb, model="iid", hyper=hcprior)+f(ves_eff, model="iid", hyper=hcprior)+f(w, model=spde, group=w.group, control.group=list(model="ar", order=4, hyper=h.spec))+log(hooks/1000)	ZIP	Log	Doropped HPB=3 and 7 (n=2 sets), Selected model, Data was aggregated by yr, qtr, lat, lon, hpb, and vessel name. Calculation was stopped because of time limitation
11	1994-2009	zip_sptime_yr	swo~-1+yr+f(ves_eff, model='iid',hyper=hcprior)+f(w, model=spde, group=w.group, control.group=list(model='ar1', hyper=h.spec))+log(hooks/1000)	ZIP	Log	Data was aggregated by yr, qtr, lat, lon, hpb, and vessel name. Proposed model
12	1994-2009	zip_sptime_yrqtrhpb2	swo~-1+yr+qtr+f(hpb, model='iid', hyper=hcprior)+f(w, model=spde, group=w.group, control.group=list(model='ar1', hyper=h.spec))+log(hooks/1000)	ZIP	Log	Data was aggregated by yr, qtr, lat, lon, hpb, and vessel name.
13	1994-2009	zip_sptime_yrqtrves	swo~-1+yr+qtr+f(ves_eff, model="iid", hyper=hcprior)+f(w, model=spde, group=w.group, control.group=list(model="ar1", hyper=h.spec))+log(hooks/1000)	ZIP	Log	Data was aggregated by yr, qtr, lat, lon, hpb, and vessel name.
14	1994-2009	zip_sptime_allcov1	swo~-1+yr+qtr+hpb+f(ves_eff, model='iid', hyper=hcprior)+f(w, model=spde, group=w.group, control.group=list(model='ar1', hyper=h.spec))+log(hooks/1000)	ZIP	Log	Data was aggregated by yr, qtr, lat, lon, hpb, and vessel name.
15	1994-2009	zip_sptime_allcov2	swo~-1+yr+qtr+f(hpb, model='iid', hyper=hcprior)+f(ves_eff, model='iid', hyper=hcprior)+f(w, model=spde, group=w.group, control.group=list(model='ar1', hyper=h.spec))+log(hooks/1000)	ZIP	Log	Data was "not" aggregated
16	1994-2009	zip_sptime_allcov3	swo~-1+yr+qtr+hpb+f(ves_eff, model='iid', hyper=hcprior)+ f(w, model=spde, group=w.group, control.group=list(model='ar1', hyper=h.spec))+f(w2, model=spde, group=w2.group, control.group=list(model="iid"))+log(hooks/1000), w=year, w2=season	ZIP	Log	Data was aggregated by yr, qtr, lat, lon, hpb, and vessel name.
17	1976-1993	zip_spqtr_yr	swo~-1+yr+f(ves_eff, model="iid", hyper=hcprior)+f(w, model=spde, group=w.group, control.group=list(model="iid"))+log(hooks/1000), w=qtr	ZIP	Log	Data was aggregated by yr, qtr, lat, lon, hpb, and vessel name.
18	1976-1993	zip_sptime_simple	swo~-1+yr+f(w, model=spde, group=w.group, control.group=list(model='ar1', hyper=h.spec))+log(hooks/1000)	ZIP	Log	Data was aggregated by yr, qtr, lat, lon, hpb, and vessel name. Proposed model Drop 200<d$swo
19	1976-1993	zip_sptime_yr	swo~-1+yr+f(ves_eff, model='iid',hyper=hcprior)+f(w, model=spde, group=w.group, control.group=list(model='ar1', hyper=h.spec))+log(hooks/1000)	ZIP	Log	Data was aggregated by yr, qtr, lat, lon, hpb, and vessel name.
20	1976-1993	zip_sptime_yr_rev1	swo~-1+yr+f(ves_eff, model='iid',hyper=hcprior)+f(w, model=spde, group=w.group, control.group=list(model='ar1', hyper=h.spec))+log(hooks/1000)	ZIP	Log	Data was aggregated by yr, qtr, lat, lon, hpb, and vessel name. Drop 200<d$swo
21	1976-1993	zip_sptime_allcov2	swo~-1+yr+qtr+f(hpb, model='iid', hyper=hcprior)+f(ves_eff, model='iid', hyper=hcprior)+f(w, model=spde, group=w.group, control.group=list(model='ar1', hyper=h.spec))+log(hooks/1000)	ZIP	Log	Data was aggregated by yr, qtr, lat, lon, hpb, and vessel name.
22	1976-1993	zip_sptime_allcov1	swo~-1+yr+qtr+hpb+f(ves_eff, model='iid', hyper=hcprior)+f(w, model=spde, group=w.group, control.group=list(model='ar1', hyper=h.spec))+log(hooks/1000)	ZIP	Log	Data was aggregated by yr, qtr, lat, lon, hpb, and vessel name.
23	1976-1993	zip_sptime_yrqtrves	swo~-1+yr+qtr +f(ves_eff, model="iid", hyper=hcprior)+f(w, model=spde, group=w.group, control.group=list(model="ar1", hyper=h.spec))+log(hooks/1000)	ZIP	Log	Data was aggregated by yr, qtr, lat, lon, hpb, and vessel name.
24	1976-1993	zip_sptime_allcov3	swo~-1+yr+qtr+hpb+f(ves_eff, model='iid', hyper=hcprior)+f(w, model=spde, group=w.group, control.group=list(model='ar1', hyper=h.spec))+f(w2, model=spde, group=w2.group, control.group=list(model="iid"))+log(hooks/1000), w=year, w2=season	ZIP	Log	Data was aggregated by yr, qtr, lat, lon, hpb, and vessel name.

TABLE 2. Model description for the mean body weight of swordfish caught by Japanese longline fishery.

No	Time period	Model name	Model description in R-INLA	Distribution	Link	Remarks
1	2010-2019	mean_bw	mean_bw~-1+yr+qtr+hpb+f(ves_eff, model='iid', hyper=hcprior)+f(w, model=spde, group=w.group, control.group=list(model='ar1', hyper=h.spec))	Log Normal	Identity	Data was "not" aggregated Dropped HPB=3 and 7 (n=2 sets), Selected model
2	1994-2009	mean_bw	mean_bw~-1+yr+f(ves_eff, model='iid',hyper=hcprior)+f(w, model=spde, group=w.group, control.group=list(model='ar1', hyper=h.spec))	Log Normal	Identity	Data was aggregated by yr, qtr, lat, lon, hpb, and vessel name

TABLE 3. Information criterion table for the abundance index models.

No	Time period	Model name	waic	loocv	Dispersion	Estimated Zero Prob
1	2010-2019	po_sptime_yrqtr	632607	632726	2.37	
2	2010-2019	po_sptime_allcov	631567	631660	2.36	
3	2010-2019	zip_sptime_yr	638880	639007	1.78	
4	2010-2019	zip_sptime_allcov1	621141	621086	1.81	
5	2010-2019	zip_sptime_allcov1_rev1	616690	616796	1.7	0.092
6	2010-2019	zip_sptime_allcov2	NA	621588	2.03	
7	2010-2019	zip_sptime(ar4)_allcov	-	-	-	
8	2010-2019	zip_sptime_allcov3	Not yet	Not yet	Not yet	
9	2010-2019	zip_sptime_allcov1_rev2	Not yet	Not yet	Not yet	
10	2010-2019	zip_sptime(ar4)_allcov_rev1	-	-	-	
11	1994-2009	zip_sptime_yr	716793	715734	1.62	0.1
12	1994-2009	zip_sptime_yrqtrhpb2	737366	NA	1.73	
13	1994-2009	zip_sptime_yrqtrves	Crush	Crush	Crush	
14	1994-2009	zip_sptime_allcov1	Not yet	Not yet	Not yet	
15	1994-2009	zip_sptime_allcov2	Crush	Crush	Crush	
16	1994-2009	zip_sptime_allcov3	Not yet	Not yet	Not yet	
17	1976-1993	zip_spqtr_yr	1329895	1317873	2.1	
18	1976-1993	zip_sptime_simple	1286971	1282804	1.71	0.15
19	1976-1993	zip_sptime_yr	Crush	Crush	Crush	
20	1976-1993	zip_sptime_yr_rev1	Crush	Crush	Crush	
21	1976-1993	zip_sptime_allcov2	Crush	Crush	Crush	
22	1976-1993	zip_sptime_allcov1	Not yet	Not yet	Not yet	
23	1976-1993	zip_sptime_yrqtrves	Not yet	Not yet	Not yet	
24	1976-1993	zip_sptime_allcov3	Not yet	Not yet	Not yet	

TABLE 4. Information criterion table for the mean body weight models.

No	Time period	Model name	waic	loocv	Dispersion	Estimated Zero Prob
1	2010-2019	mean_bw	153250	153250	-	-
2	1994-2009	mean_bw	160187	160188	-	-